International Journal of Heat and Mass Transfer 62 (2013) 362–372

Contents lists available at SciVerse ScienceDirect

International Journal of Heat and Mass Transfer

journal homepage: www.elsevier.com/locate/ijhmt

Effects of local geometry and boundary condition variations on transpiration cooling

Yuan-Qing Liu [a,b,c], Yan-Bin Xiong [a,b], Pei-Xue Jiang [a,b,*], Yang-Ping Wang [a,b], Ji-Guo Sun [d]

[a] Key Laboratory for Thermal Science and Power Engineering of Ministry of Education of China, Beijing, China
[b] Beijing Key Laboratory of CO_2 Utilization and Reduction Technology, Department of Thermal Engineering, Tsinghua University, Beijing 100084, China
[c] Beijing Institute of Astronautical System Engineering, Beijing 100076, China
[d] Beijing Aerospace Propulsion Institute, Beijing 100076, China

ARTICLE INFO

Article history:
Received 22 August 2011
Received in revised form 29 November 2012
Accepted 17 February 2013
Available online 9 April 2013

Keywords:
Transpiration cooling
Boundary condition variation
Local thermal non-equilibrium model

ABSTRACT

The influences of the thermal conductivity and porosity of the porous wall and locally extraordinarily high heat fluxes on the hot surface and the location of a low porosity region within one and two layer porous walls on the temperature field were analyzed numerically. The local thermal non-equilibrium model was used to predict the temperature distributions in the solid and phases within a 2-D computational domain. The predicted results show that the porosity and thermal conductivity of the top layer significantly influence the temperature distribution of the solid matrix when the hot surface is subjected to uniform or locally extraordinarily high heat flux boundary conditions. In addition, the study shows that the location of the low porosity region also significantly affects the temperature field in the two layer model consisting of a bronze matrix and a ceramic coating.

1. Introduction

The thermal loads experienced by rocket thruster walls, hypersonic vehicle surfaces and gas turbine blades are so high that without proper cooling the temperatures of key components will far exceed the melting point of the metal and the life times of these components will be dramatically shortened. Transpiration cooling has been proven to be an efficient and promising cooling technique which can cool the throat regions of rocket nozzles, injector heads of rocket engines, gas turbine blades and combustion chamber liners. With a porous wall, the coolant is driven through the random pores inside the porous media to remove heat by convective heat transfer. As the coolant flows out of the hot side of the porous wall, it spreads laterally downstream to generate a protective gas film to prevent surface damage from the extremely hot main stream.

The local thermal non-equilibrium model is often used to obtain more accurate temperature distributions of the solid and fluid phases within porous media. A comprehensive comparison of the models for heat and mass transport through porous media was performed by Alazmi and Vafai [1], Amiri and Vafai [2], Amiri et al. [3] and Vafai and Kim [4] with the effects of various parameters, including the Darcy number, inertia parameter, Reynolds number, porosity, particle diameter, and fluid-to-solid conductivity analyzed with the local thermal non-equilibrium model. The numerical results of Jiang and Lu [5,6], Jiang et al. [7–9], which were validated by comparisons with experimental data, showed that convection heat transfer in porous media can be accurately predicted by the local thermal non-equilibrium model with proper boundary conditions. Shi and Wang [10,11] Wang and Shi [12] Wang and Wang [13] used the local thermal non-equilibrium model to study ablation and transpiration cooling.

Ceramic matrices can withstand high temperatures and reduce coolant consumption due to their much higher melting points in contrast to sintered metal porous media. Therefore, ceramics are already widely used as gas turbine blade thermal barrier coatings applied using the thermal spray technique. Recently, some new designs have been proposed to extend the cooling performance using transpiration materials and structures, such as matrices made of two porous layers. The base layer is a metallic porous medium serving as the structural matrix due to the good mechanical strength while the top layer is a ceramic porous material serving as a thermal barrier coating. Von Wolfersdorf [14] studied the influence of the volumetric heat transfer coefficient and the thermal conductivity of the top layer and pointed out that this structure can be applied to the cooling of gas turbine combustor liners. Shi and Wang [15] optimized a two layer porous structural for transpiration cooling using an intelligent genetic algorithm based on a simplified local thermal non-equilibrium model and proposed a structural design method that optimizes several factors

* Corresponding author at: Beijing Key Laboratory of CO_2 Utilization and Reduction Technology, Department of Thermal Engineering, Tsinghua University, Beijing 100084, China. Tel.: +86 10 62772661; fax: +86 10 62770209.
E-mail address: Jiangpx@tsinghua.edu.cn (P.-X. Jiang).

0017-9310/$ - see front matter © 2013 Elsevier Ltd. All rights reserved.
http://dx.doi.org/10.1016/j.ijheatmasstransfer.2013.02.075

Nomenclature

a_{sf}	specific surface, [m^{-1}]
d_p	mean particle diameter, [m]
D	hydraulic diameter of the channel
h_{sf}	fluid-to-solid heat transfer coefficient, [W/m^2 K]
H	porous wall thickness, [m]
K	porous media permeability, [m^2]
M	mass flow rate, [kg/s]
q	heat flux, [W/m^2]
Re	Reynolds number, $\rho u D/\mu$
T	temperature, [K]
u	velocity in the x direction, [m/s]
u_p	pore velocity in the x direction, [m/s]
v_p	pore velocity in the y direction, [m/s]
Up	absolute pore velocity ($Up = \left(u_p^2 + v_p^2\right)^{1/2}$), [m/s]
x, y	coordinates, [m]
W	width of computational domain, [m]
Greek symbols	
ε	porosity
λ	thermal conductivity, [W/(m K)]
λ_d	additional thermal conductivity due to thermal dispersion, [W/(m K)]
ρ	density, [kg/m^3]
μ	absolute viscosity, [Pa/s]
μ_e	effective absolute viscosity ($\approx\mu_f$), [Pa/s]
Subscript	
c	coolant
d	dispersion
eff	effective property
f	fluid phase
p	particle
s	solid phase

including the composition, porosity and thickness of each layer. This design is expected to more conveniently and flexibly control the temperature distribution throughout the porous wall.

However, all these previous studies with two-equation models [10–15] were based on analytical solutions of a simplified, one-dimensional, local thermal non-equilibrium model that neglected the thermal conduction in the gaseous coolant and the thermal dispersion inside the solid matrix. In practical applications using transpiration cooling, the geometry and the boundary conditions are very complicated and non-uniform, some areas have ultra high heat fluxes and some of the porous matrix can become blocked leading to deviations from the one-dimensional assumption.

The present study uses a 2-D rectangular porous model with one or two porous layers for transpiration cooling to analyze the influence of the porous wall properties and boundary condition on the heat transfer within the porous zone using the local thermal non-equilibrium model. The study analyzes the effect of the thermal conductivity and porosity of the top layer, locally extraordinarily high heat fluxes on the hot surface and the location of a low porosity region in the wall on the temperature field.

2. Physical–mathematical model and modeling method

A schematic diagram of the physical model is given in Fig. 1. The coolant flowed upward through the porous zone from the coolant reservoir with a bulk temperature, T_c. There was convective heat transfer with a heat transfer coefficient, h_c, to the cold surface, with a constant or variable heat flux imposed on the solid matrix at the hot surface. The left and right vertical boundaries were assumed to be impermeable and thermally insulated. The physical model was 60 mm wide and 5 mm high with the porous region modeled as either a single layer or as two layers.

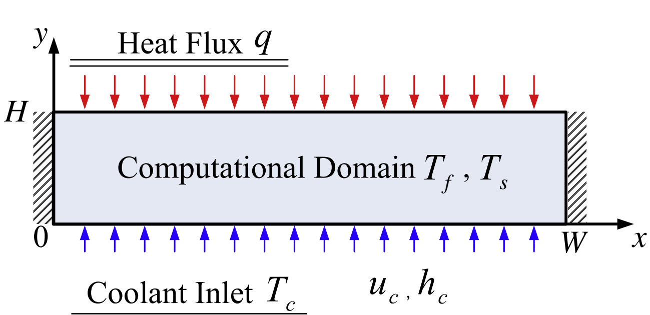

Fig. 1. Sketch of the physical model.

As shown in Table 1, the top layer in the two layer model was 2 mm thick while the base layer was 3 mm thick. The study analyzes the influence of the thermal conductivity and porosity variations of the top layer on the solid and fluid phase temperature distributions within the computational domain. The top layer solid thermal conductivity was assumed to be λ_s = 2 W/m K or λ_s = 20 W/m K, while the base layer solid thermal conductivity was assumed to be 75 W/m K. The top layer porosity was assumed to be ε = 0.1 or ε = 0.6, while the base layer porosity was assumed to be 0.3.

In addition, the heat transfer characteristics were analyzed with a low porosity region in the system using a sintered bronze particle bed as the structural base matrix with a ceramic coating layer on top. The top layer in this model was 1 mm thick while the base layer was 4 mm thick. The low porosity region was assumed to have a porosity of 0.05 and a thermal conductivity of 2 W/m K in the ceramic layer and 75 W/m K in the bronze layer. Four geometries with different block locations were analyzed to study the effect of the block location on the temperature field. The detailed geometric information is listed in Table 2.

The flow was assumed to be two-dimensional and compressible with the Darcy–Forchheimer–Brinkman equation used to describe the fluid flow within the computational domain. Due to the large temperature differences in the fluid phase between the entrance and the exit of the porous zone, the physical property variations with temperature of the fluid phase were calculated based on the NIST database. The steady-state volume averaged governing equations for the local thermal non-equilibrium conditions are [5–8]:

Continuity equation

$$\frac{\partial(\rho_f \varepsilon u_p)}{\partial x} + \frac{\partial(\rho_f \varepsilon v_p)}{\partial y} = 0 \tag{1}$$

Momentum equation

$$\frac{\partial(\rho_f \varepsilon u_p u_p)}{\partial x} + \frac{\partial(\rho_f \varepsilon v_p u_p)}{\partial y} = -\frac{\partial(\varepsilon p_p)}{\partial x} + \frac{\partial}{\partial x}\left(\varepsilon\mu_e \frac{\partial u_p}{\partial x}\right) + \frac{\partial}{\partial y}\left(\varepsilon\mu_e \frac{\partial u_p}{\partial y}\right) - \frac{\mu_f}{K}\varepsilon^2 u_p - \varepsilon^3 \frac{\rho_f F}{\sqrt{K}}|U_p|u_p \tag{2}$$

$$\frac{\partial(\rho_f \varepsilon u_p v_p)}{\partial x} + \frac{\partial(\rho_f \varepsilon v_p v_p)}{\partial y} = -\frac{\partial(\varepsilon p_p)}{\partial y} + \frac{\partial}{\partial x}\left(\varepsilon\mu_e \frac{\partial v_p}{\partial x}\right) + \frac{\partial}{\partial y}\left(\varepsilon\mu_e \frac{\partial v_p}{\partial y}\right) - \frac{\mu_f}{K}\varepsilon^2 v_p - \varepsilon^3 \frac{\rho_f F}{\sqrt{K}}|U_p|v_p \tag{3}$$